PAPER

Check for updates

Non-covalent interactions between sertraline stereoisomers and 2-hydroxypropyl-β-cyclodextrin: a quantum chemistry analysis†

Joanatan-Michael Bautista-Renedo,[a] Erick Cuevas-Yañez,[a] Horacio Reyes-Pérez,[c] Rubicelia Vargas, [b] Jorge Garza [b] and Nelly González-Rivas [*a]

Inclusion compounds formed between sertraline stereoisomers and β-cyclodextrin, and 2-hydroxypropyl-β-cyclodextrin, were analyzed by using quantum chemistry methods. The exploration of the potential energy surface was performed using chemical intuition and classical molecular mechanics. This approach delivered around 200 candidates for low energy adducts, which were optimized through the PBE0/6-31G(d,p) method, and after this process solvent effects were considered by the continuous solvent model. This analysis showed that β-cyclodextrin and 2-hydroxypropyl-β-cyclodextrin are good trappers of sertraline, although the isomers suggested by molecular dynamics presented higher binding energies than those obtained by chemical intuition. The role of hydrogen bonds in the formation of adducts was studied using the non-covalent interactions index and the quantum theory of atoms in molecules. In this article we concluded that these interactions are present in all adducts, however, they are not important in the stabilization of these inclusion compounds. The molecular electrostatic potential indicates that Coulomb interactions could be responsible for the formation of these systems, although sophisticated solvent models must be used to confirm this conclusion, which are impractical in this case because of the sizes involved in these systems.

1 Introduction

Sertraline (*cis*-(1*S*,4*S*)-4-(3,4-dichlorophenyl)-*N*-methyl-1,2,3,4-tetrahydronaphthalen-1-amine) is an important inhibitor of serotonin, with remarkable antidepressant characteristics.[1,2] The relevance of this compound is evidenced by the sales observed in the pharmaceutical industry for the treatment of obsessive–compulsive disorder, panic disorder or social anxiety disorder.[3,4] The chemical structure of sertraline (SRT), depicted in Fig. 1, contains one amino group, three rings (two aromatic and one aliphatic) plus two chiral centers, which yield 4 stereoisomers: *cis*-(1*S*,4*S*)-SRT, *cis*-(1*R*,4*R*)-SRT, *trans*-(1*R*,4*S*)-SRT, and *trans*-(1*S*,4*R*)-SRT. In this article, we will refer to these stereoisomers as **I**, **II**, **III** and **IV**, respectively. Curiously, only stereoisomer **I** exhibits the desired biological activity, which is

another example of chiral molecules involved in pharmaceutical analysis that represent challenges to separation methods since only this stereoisomer must be favored in industrial processes.[5] Naturally, the remaining stereoisomers can be found as impurities and consequently knowledge of the molecular interactions involved in separation methods is crucial for improving the efficiency of such processes.

One of the most used separation methods is high-performance liquid chromatography with β-cyclodextrin (βCD), presented in Fig. 2a, and derivatives of it.[6–8] It is well

ᵃCentro Conjunto de Investigación en Química Sustentable UAEM-UNAM, km 14.5 carretera Toluca-Atlacomulco, Campus UAEMex "El Rosedal" San Cayetano-Toluca de Lerdo, Toluca de Lerdo, Estado de México, C. P. 50200, Mexico. E-mail: nmdgonzalezr@uaemex.mx

ᵇDepartamento de Química, División de Ciencias Básicas e Ingeniería, Universidad Autónoma Metropolitana-Iztapalapa, San Rafael Atlixco 186, Col. Vicentina. Iztapalapa, México D. F., C. P. 09340, Mexico. E-mail: jgo@xanum.uam.mx

ᶜTecnológico de Estudios Superiores de Jocotitlán, Carretera Toluca-Atlacomulco KM 44.8 Ejido de San Juan y, San Agustin, C.P. 50700 Jocotitlán, Mexico

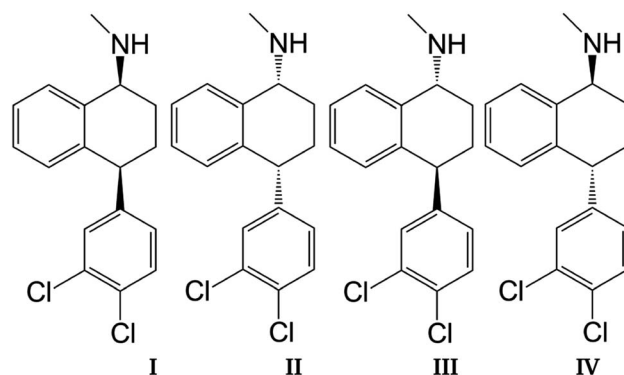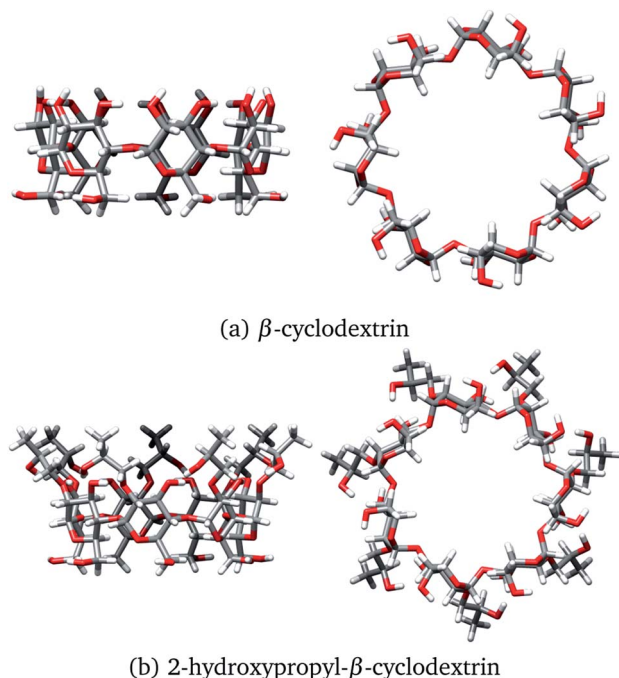† Electronic supplementary information (ESI) available. See DOI: 10.1039/c9ra10218c

Fig. 1 Sertraline stereoisomers: (I) *cis*-(1*S*,4*S*), (II) *cis*-(1*R*,4*R*), (III) *trans*-(1*R*,4*S*), (IV) *trans*-(1*S*,4*R*).

(a) β-cyclodextrin

(b) 2-hydroxypropyl-β-cyclodextrin

Fig. 2 Two views of (a) β-cyclodextrin and (b) 2-hydroxypropyl-β-cyclodextrin. Both structures were optimized with the PBE0/6-31G(d,p) method.

recognized that cyclodextrins (CDs) are convenient for forming inclusion compounds due to the toroidal form acquired when glucopyranose units are linked to form a ring. Typically, these CDs contain 6, 7, or 8 glucopyranose units, labeled as α, β, or γ, respectively.[9] In some cases, the molecular characteristics exhibited by CDs are used to separate stereoisomer mixtures by forming diastereomeric complexes through host–guest chemistry.[10,11] It is worth noting that the hydroxyl groups of CDs increase the solubility of the host, inducing additional sites to interact with the corresponding enantiomer, and improving the chiral recognition.[12,13]

From a theoretical viewpoint, classical molecular dynamics predominates over quantum chemistry techniques for the study of CD inclusion compounds.[14] The reason is clear: a high computational effort is required to study the electronic structures of these systems. Passos *et al.* proposed some inclusion complexes between βCD and stereoisomer **I** by using two supramolecular models: βCD:**I** and βCD:**I**:βCD. In this study, the potential energy surface (PES) was explored using structures built by chemical intuition and by evaluating the total energy with the PM3 semi-empirical method. For the molecular structure with the lowest PM3 energy, the PBE1PBE/6-31G(d,p) method was used without solvent effects.[15] The main conclusion of this study is that the interactions between βCD and **I** arise from the amino and hydroxyl groups. Unfortunately, this study was not in accordance with the experimental information; for this reason, a few of the authors of the report recomputed the supramolecular models including water molecules.[16] In this study, the PBE0/6-31G(d,p) method was used to analyze the electronic structures of these systems. In both studies, there are

some crucial conclusions: (1) the primary host–guest interactions involve the amino group and take place outside the cavity, and (2) βCD exhibits no important structural distortions when it forms adducts, compared with the isolated system. This result is strange since such distortions are observed in inclusion adducts. For example, αCD shows deformations when dimethylformamide is enclosed within its cavity,[17] and deformations are also observed when 4-dimethylamino-benzonitrile forms an inclusion adduct with βCD.[18]

At this point, we have explained that βCD has been used to form inclusion compounds, in particular with SRT. However, there are reports where this CD is functionalized to improve its trapping capacity. 2-hydroxypropyl-β-cyclodextrin (HPβCD), depicted in Fig. 2b, is an example of a functionalized CD, which has been used for several applications.[19–25] This functionalized CD is obtained by replacing all the secondary alcohols in βCD with 2-hydroxypropyl groups. From a theoretical viewpoint, some structures for the HPβCD:**I** system have been proposed by using chemical intuition.[21] To the best of our knowledge, the interactions involved in βCD:SRT adducts, especially which interactions control the behavior of these systems, have not been characterized through quantum chemistry methods. Thus, the aim of this article is twofold. First, we study the capacity of βCD and HPβCD to trap SRT stereoisomers, and second, the interactions that drive the stabilization of βCD:SRT and HPβCD:SRT adducts are analyzed by using several scalar and vector fields developed in quantum chemistry.

2 Methods

The starting point of this study was a βCD structure obtained by X-ray diffraction.[26] We removed the water molecules from the cif file and from this structure we built the HPβCD structure. For SRT, we started with the SRT·HCl compound characterized by X-ray diffraction,[27] since this compound is known experimentally. For this reason, we work with the protonated form, SRT·H$^+$, because this species is found in aqueous medium. This procedure was used for the *cis*-(1S,4S) SRT stereoisomer and from this structure we built the rest of the stereoisomers. All these structures were optimized with the PBE0/6-31G(d,p) method, and they were true minima since we checked them using a frequency analysis. Eight inclusion compounds were proposed by looking for favorable contacts between SRT and βCD, testing both sides of the toroidal structure of βCD. These structures were the starting point for classical molecular dynamics (MD) simulations with the Tinker code v8.4 (ref. 28) and the MM3 force field. We carried out this simulation at a temperature of 298 K and an interval of 100 000 ps. From this simulation we took snapshots of all structures within a window of relative energies defined between 0 and 10 kcal mol^{-1}. With this procedure we obtained around 200 structures. The main reason for this approach was the fact that exploration of the PES was of interest to us, not the average thermodynamic properties. The final structures obtained by MD were optimized with the PBE0/6-31G(d,p) method. It is worth noting that some structures were structurally similar, and for that reason, we used unique structures. All these electronic structure

calculations were performed with the Terachem suite code v1.9.[29,30] From here, we used those structures with relative energies less than 5 kcal mol^{-1}. Binding energies were estimated in the gas phase and in solution through the COSMO model implemented in Terachem by using the structure of the gas phase and performing a single point calculation with a dielectric constant $\varepsilon = 78.4$ for COSMO. The non-covalent interactions index (NCI)[31] was used to explore the contacts involved in each inclusion compound and the characterization of each contact was carried out using the quantum theory of atoms in molecules (QTAIM).[32,33] All these calculations were done using the graphics processing units for atoms and molecules (GPUAM) code.[34,35] The molecular electrostatic potential (MEP) was evaluated by using a new implementation of this property over graphics processing units.[36] The approach used for βCD adducts was also applied to find HPβCD:SRT structures.

3   Results

The exploration of the PES for inclusion compounds of CDs is an issue in quantum chemistry because sometimes the size of such systems is forbidden by several quantum chemistry methods. For that reason, in this article, we used classical MD techniques to explore the PES. Besides, some inclusion compounds were proposed by inserting SRT in different orientations on both sides of βCD and trying to form hydrogen bonds. In this article, this procedure will be referred to as chemical intuition, and the structures proposed in this way are presented in Fig. 3.

3.1   βCD as a trapper of sertraline

As a starting point, we will analyze inclusion compounds between βCD and stereoisomer **I**. For this discussion, we will remark on the results obtained for adducts proposed by chemical intuition (CI) and MD since in many reports CI is the only way to analyze these systems. Remember that each structure obtained with these two approaches was optimized with the PBE0/6-31G(d,p) method. We report in Fig. 4 the three most stable adducts found by each approach, where CI and MD indicate chemical intuition and molecular dynamics, respectively. The coordinates of these structures are reported in the ESI† where we report more adducts found by CI and MD. A rapid comparison between our structures and those reported in the literature shows that βCD:**I**_CI3 is quite similar to that reported by Passos.[15] We want to mention that the structures provided by MD differ appreciably from those optimized by DFT, mainly where there are hydrogen bonds, since some parts of the CDs do not show important deviations, particularly where hydrogen bonds are not present. Table S1 in the ESI† presents some results of the comparison between MD and optimized structures.

For the six adducts in Fig. 4, the corresponding binding energies in the gas phase,

$$\Delta E_{\mathrm{g}} = E_{\mathrm{adduct}}^{\mathrm{opt}} - E_{\mathrm{CD}}^{\mathrm{opt}} - E_{\mathrm{SRT}}^{\mathrm{opt}}, \tag{1}$$
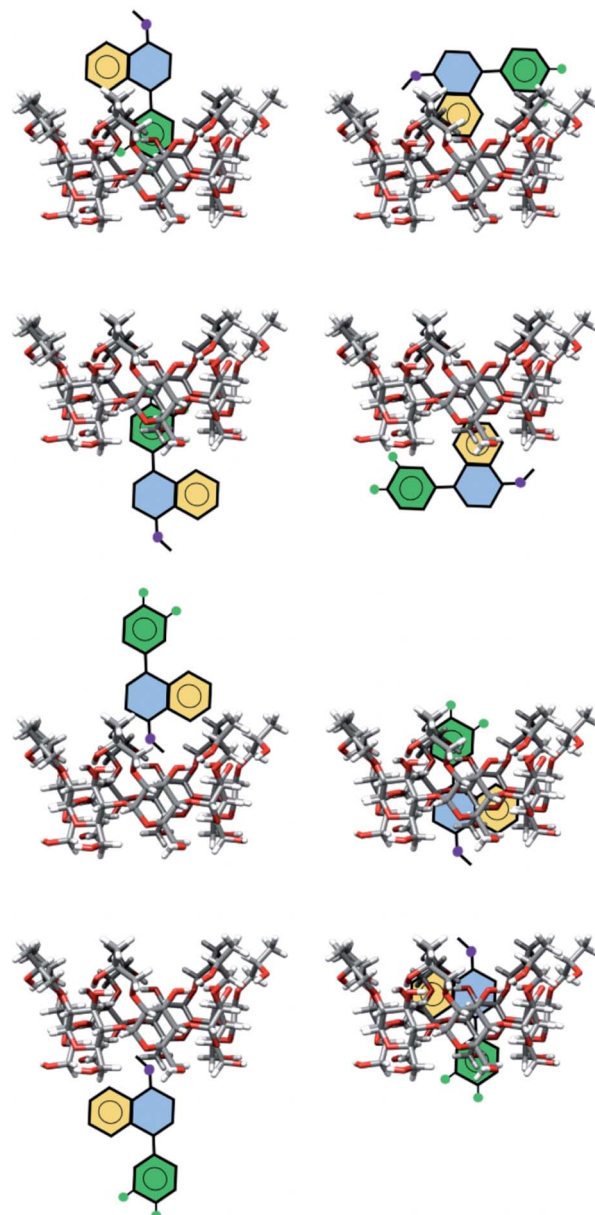

Fig. 3 Schematic representation of geometries of inclusion compounds formed between βCD and sertraline stereoisomer I proposed by chemical intuition .

are reported in Table 1, and contain the zero point energy for all cases discussed in this article. In this equation E^{opt} represents the energy of the optimized structure of each isolated system, adduct and fragment. For CD and SRT, the structures obtained from X-ray diffraction were optimized. All structures are reported in the ESI.† The first result we notice in this table is the large difference between the structures built by CI and those obtained from MD, since MD delivers adducts with binding energies much larger than those obtained using chemical intuition. We want to stress the binding energy obtained for structure βCD:**I**_CI3 since this structure gives the lowest binding energy among the adducts considered in this work, and this binding energy is similar to that reported by Passos and
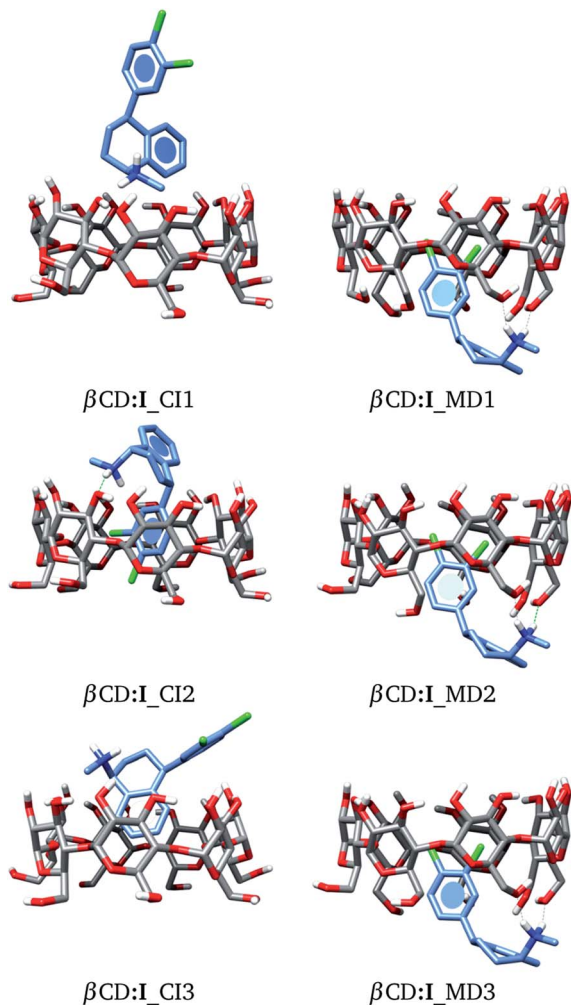
Fig. 4 Three lowest-lying βCD:I adducts obtained from proposals made by chemical intuition (CI) and molecular dynamics (MD). Final structures obtained with the PBE0/6-31G(d,p) method.

Table 1 Deformation and association energies for three βCD:I adducts found by chemical intuition and molecular dynamics. Deformation energies correspond only to βCD, and association energies correspond to adducts in the gas phase (ΔE_g, ΔG_g), and in water (ΔE_s, ΔG_s). All energies were calculated by using the PBE0/6-31G(d,p) method. ΔE contains the zero point energy and the Gibbs energy was estimated at $T = 298.15$ K. All quantities are in kcal mol^{-1}

Adduct	ΔE_g	ΔG_g	ΔE_s	ΔG_s	ΔE_{def}
Chemical intuition					
βCD:**I**_CI1	−25.0	−10.6	−8.8	5.6	10.3
βCD:**I**_CI2	−24.8	−7.0	−5.3	12.5	11.2
βCD:**I**_CI3	−18.4	−1.0	−4.7	12.6	6.0
Molecular dynamics					
βCD:**I**_MD1	−44.8	−25.0	−11.8	7.9	14.8
βCD:**I**_MD2	−41.7	−22.9	−12.6	6.2	4.5
βCD:**I**_MD3	−41.5	−23.2	−13.1	5.3	14.5

models must be considered, but the size of our systems implies an enormous task.

Clearly MD proposes molecular structures that present large binding energies. In principle, this result must be mapped over the geometrical structures in these systems, in particular over the cone formed in βCD. To explore this idea, we used an energy contribution that takes into account the deformation of βCD when it creates the corresponding adduct. This term is defined as

$$\Delta E_{def} = E_{CD}^{adduct} - E_{CD}^{opt}, \qquad (2)$$

where E_{CD}^{adduct} corresponds to the energy of the βCD structure within the adduct in the gas phase and E_{CD}^{opt} is already defined above.[37,38] If $\Delta E_{def} \approx 0$ then the βCD structure shows small changes with respect to the isolated structure, and large values of this energy difference represent considerable distortions in the βCD structure. In this way, we can give a measure of the deformation suffered by βCD, and derivatives of it, in the adduct formation. As we can observe from Table 1, this energy change is appreciable. From these results it is evident that the MD structures exhibit the highest ΔE_{def}. We conclude from these results that MD is required to study βCD:**I** inclusion compounds since this technique considers thermal effects, which induce deformations in βCD through the kinetic energy of the system, and consequently high binding energies are observed. To corroborate this conclusion we explored the βCD:**I** PES by using an implementation of the simulated annealing method reported recently.[39] Using this method we found adducts with similar binding energies to those obtained by chemical intuition. This is a significant result for studying inclusion compounds of βCD since the crucial part of MD is not just the stochastic procedure intrinsic to this method, but the movement of all atoms involved in the system is relevant, and this is the main difference compared to other stochastic methods. Thus, MD is recommended for obtaining high binding energies for βCD:**I** inclusion compounds. The presence of large structural deformations is not sufficient to obtain large binding energies, as we can confirm for the βCD:**I**_MD2 adduct,

coworkers (−14.48 kcal mol^{-1}).[15] Therefore, the structures reported by Passos *et al.* do not necessarily represent the most stable structures for these systems. In the same table, we report the Gibbs energy at $T = 298.15$ K. From these results, the impact of entropic contributions is evident since they drastically reduce the binding energies at this temperature, but even with this reduction these energies indicate stable adducts. As we mentioned in the Methods section, solvent effects were estimated through a dielectric continuum model and the corresponding results (ΔE_s and ΔG_s) are also reported in Table 1. It is clear that solvent effects have an important role in the binding energies of these adducts, which is related to the polar species involved in these systems. From these results it is clear that solvent effects decrease the binding energies, and these effects are bigger than those caused by entropy. If we consider $T = 298.15$ K and solvent effects, our methodology predicts unstable adducts, for at lower temperatures we obtained negative Gibbs energy changes. It is known that solvent effects cause problems for charged species and for this reason these effects dramatically increase ΔE_s and ΔG_s. A mix between explicit and implicit

which presents the lowest ΔE_{def} with a large ΔE_g. However, MD gives many possibilities for structural arrangements, and for that reason we propose a protocol for studying βCD inclusion compounds: (initial structures) → MD → (DFT optimization).

The interactions involved in βCD inclusion compounds are interesting since, in principle, they induce the most stable structures. To understand the intermolecular interactions involved within the adducts reported here, we used the NCI to reveal the sites where weak interactions are present. In Fig. 5 we contrast the NCI (green and blue isosurfaces) for adducts proposed by CI and MD. We did this analysis for several adducts, as reported in the ESI.† The colours are as follows: (a) blue is negative, (b) green is small (close to zero), and (c) red is positive. Blue regions indicate strong attractive zones between fragments and green isosurfaces are associated with weak attractive van der Waals interactions. Red zones represent non-attractive interactions. In the same figure, the electron density, $\rho(r)$, is presented with an isosurface of $\rho(r) = 0.01$ atomic units (au). This is shown in white for βCD and orange for SRT.

From Fig. 5, a large green zone is clearly present in βCD:**I**_MD1; contrary to this behavior, in βCD:**I**_CI1, this region is small. Thus, the NCI indicates that there are more attractive interactions in the adduct proposed by MD than in that suggested by CI. Besides, in this figure the electron density helps in observing the distortions exhibited in both adducts. For this reason we used the NCI plus $\rho(r)$ to observe possible non-covalent interactions between fragments and structural distortions, in addition to ΔE_{def}.

The electron density was not only used to observe structural distortions, but was also used in the QTAIM approach, where the electron density and derivatives of it give information about a molecular system by using critical points of the scalar quantum chemistry field. In particular, bond critical points (BCPs) associated with hydrogen bonds were the main target since the electron density evaluated at these points is related to the strength of a hydrogen bond.[40] Within this approach, bond path prediction is required to check for the presence of hydrogen bonds. Thus, the electron densities evaluated at BCPs corresponding to hydrogen bonds are reported in Table 2. In the

βCD:**I**_CI1   βCD:**I**_MD1

Fig. 5 Electron density with an isosurface of 0.01 atomic units, in white for βCD and orange for SRT stereoisomer **I**. Non-covalent interaction index shown as green (weak interactions) and blue (strong interactions) isosurfaces.

Table 2 Characterization of hydrogen bonds involved in βCD:**I** adducts proposed by chemical intuition (CI) and molecular dynamics (MD). Distances are in Angstrom and angles are in degrees. The electron density evaluated at bond critical points is reported in atomic units

Adduct	Interaction	θ	R_{DA}	R_{HA}	ρ_{BCP}
Chemical intuition					
βCD:**I**_CI1	N–H···O	175.8	2.75	1.69	0.0458
βCD:**I**_CI2	N–H···O	162.1	2.78	1.77	0.0435
βCD:**I**_CI3	C–H···O	158.9	3.40	2.30	0.0129
Molecular dynamics					
βCD:**I**_MD1	N–H···O	154.8	2.74	1.76	0.0401
	N–H···O	158.2	2.70	1.69	0.0467
	O–H···C	151.2	3.62	2.75	0.0063
βCD:**I**_MD2	N–H···O	154.6	2.73	1.75	0.0406
	N–H···O	158.4	2.69	1.69	0.0467
	O–H···C	148.2	3.79	2.94	0.0051
βCD:**I**_MD3	N–H···O	154.2	2.74	1.76	0.0397
	N–H···O	156.7	2.68	1.68	0.0475
	O–H···C	145.2	3.50	2.66	0.0071

same table, some geometrical parameters that define hydrogen bonds, like donor–acceptor (R_{DA}) and hydrogen–acceptor (R_{HA}) distances, and the angle (θ) defined by D–H···A, are also reported. We can mention several results in this table. The N–H···O hydrogen bond is present in all systems analyzed in this article, and for all cases the electron density, ρ_{BCP}, exhibits similar values. It is worth noting that these values are associated with hydrogen bonds with greater strength than that presented by the O–H···O bonds between water molecules.[40] C–H···O and O–H···C hydrogen bonds are found in several adducts studied in this article; these contacts represent weak hydrogen bonds and therefore the corresponding ρ_{BCP} values are lower than that observed for the N–H···O contact.[40] From these results, we observe that the adducts obtained from MD exhibit more hydrogen bonds than those obtained by chemical intuition; this is another reason to use MD structures instead of CI proposals.

We want to finish this discussion by mentioning that in the adducts built by chemical intuition, βCD binds sertraline through external sections of the cone, and for the adducts obtained from MD, sertraline is bound by internal regions of βCD. In these situations, the hydrogen bonds in the MD adducts present geometrical parameters that are not favorable for their formation since the corresponding angles are far from linearity. This problem is balanced by the number of contacts observed in the structures proposed by MD.

3.2 Functionalized βCD as a sequestering agent for sertraline

In this article we built HPβCD:**I** adducts in the same way as βCD:**I** adducts. We started with 8 structures, similar to those presented in Fig. 3, and MD was performed on these structures. The three low-lying adducts obtained through chemical intuition and by MD are presented in Fig. 6. All these adducts are reported in the ESI.† We present the adducts obtained by chemical intuition, although HPβCD:**I**_CI2 and HPβCD:**I**_CI3
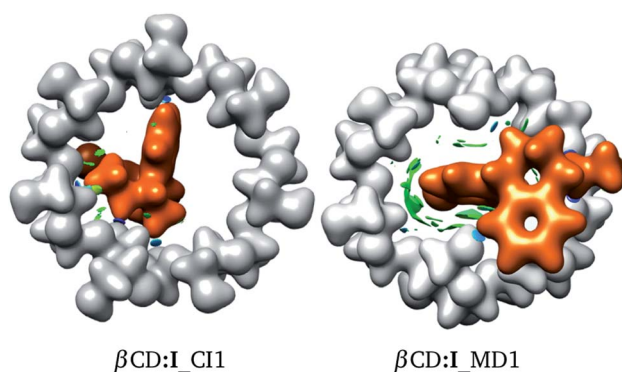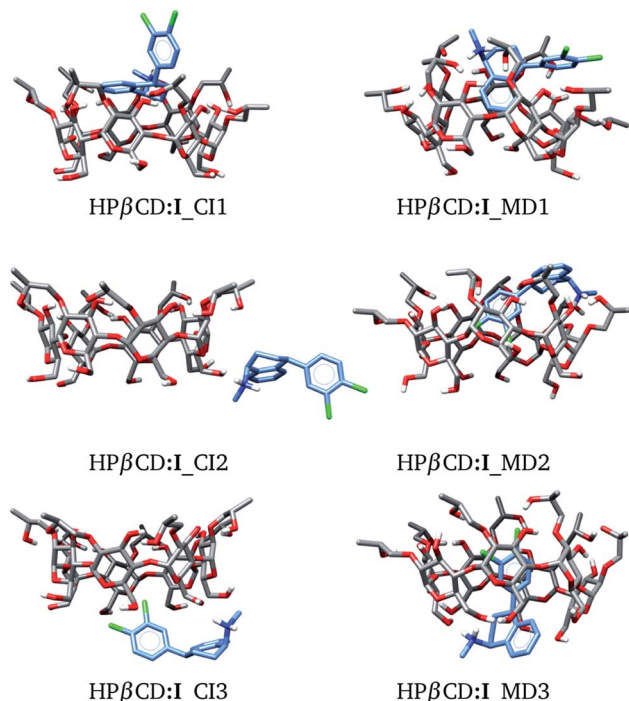
Fig. 6 Three lowest-lying HPβCD:**I** adducts obtained from chemical intuition (CI) and molecular dynamics (MD). Final structures were obtained with the PBE0/6-31G(d,p) method.

are not inclusion compounds since the SRT is outside of the cone defined by the functionalized βCD, which is evident in the figure.

The binding energies for the six adducts reported in Fig. 6 are presented in Table 3. By looking through the binding energies in the gas phase, we see an important increase in these values with respect to those observed for the βCD:**I** adducts (Table 1), suggesting that HPβCD has a higher sequestering capability to trap SRT than βCD. This is an important result since it suggests that 2-hydroxypropyl-βCD should be used instead of βCD. At $T = 298.15$ K, the Gibbs energy changes are

lower than ΔE_g, in the same way as for the βCD–SRT adducts. Besides, the MD candidates exhibit larger binding energies than those predicted by CI. Thus, MD is useful for exploring the PES in inclusion compounds of βCD or its derivatives. From Table 3 we observe that the energy changes due to deformations of HPβCD are larger than those reported for βCD. This result indicates that HPβCD is more susceptible to deformation than βCD.

For these adducts, we also evaluated the NCI in order to observe regions where these systems exhibit intermolecular contacts like hydrogen bonds or van der Waals interactions. The NCI and the electron density are exhibited in Fig. 7 for HPβCD:**I**_MD1 and HPβCD:**I**_MD2. From this figure there is no doubt about the deformation exhibited by HPβCD when this CD forms adducts with SRT; it seems that this CD encapsulates SRT, and consequently there is a large contact surface available. This result is corroborated by the NCI, which exhibits several blue and green regions between HPβCD and SRT. To give a quantitative analysis of these interactions, the QTAIM was used to characterize the hydrogen bonds. Thus, in Table 4 we report θ, R_{DA}, R_{HA} and ρ_{BCP} for these contacts.

From Table 4 we observe that the N–H···O hydrogen bond appears in all adducts considered in this article. Except for one

Fig. 7 Electron density ($\rho(r) = 0.01$ atomic units), in white for HPβCD and orange for SRT stereoisomer **I**. Non-covalent interaction index shown as green (weak interactions) and blue (strong interactions) isosurfaces. Both isomers were suggested by molecular dynamics (MD).
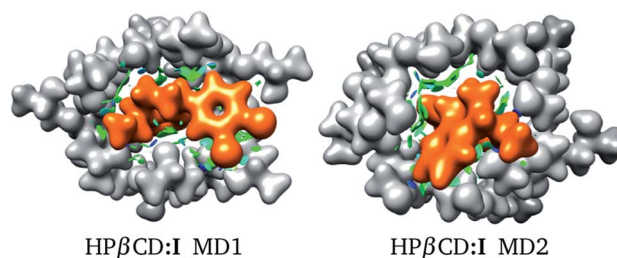
Table 3 Deformation and association energies for three HPβCD:**I** adducts found by chemical intuition and molecular dynamics. Deformation energies correspond only to HPβCD, and association energies correspond to adducts in the gas phase (ΔE_g, ΔG_g), and in water (ΔE_s, ΔG_s). All energies were calculated by using the PBE0/6-31G(d,p) method. ΔE contains the zero point energy and the Gibbs energy was estimated at $T = 298.15$ K. All quantities are in kcal mol^{-1}

Adduct	ΔE_g	ΔG_g	ΔE_s	ΔG_s	ΔE_{def}
Chemical intuition					
HPβCD:**I**_CI1	−34.7	−18.5	−12.1	4.1	6.5
HPβCD:**I**_CI2	−26.3	−11.3	−9.2	5.8	9.9
HPβCD:**I**_CI3	−26.3	−11.4	−7.0	7.9	4.9
Molecular dynamics					
HPβCD:**I**_MD1	−53.6	−33.7	−17.6	2.4	19.1
HPβCD:**I**_MD2	−51.8	−32.1	−15.4	4.2	34.9
HPβCD:**I**_MD3	−52.4	−35.0	−18.4	−0.9	19.2

Table 4 Characterization of hydrogen bonds involved in HPβCD:**I** adducts proposed by chemical intuition (CI) and molecular dynamics (MD). Distances are in Angstrom and angles are in degrees. The electron density evaluated at bond critical points is reported in atomic units

Adduct	Interaction	θ	R_{DA}	R_{HA}	ρ_{BCP}
Chemical intuition					
HPβCD:**I**_CI1	N–H···O	161.4	2.74	1.72	0.0389
HPβCD:**I**_CI2	N–H···O	171.8	2.73	1.69	0.0398
HPβCD:**I**_CI3	N–H···O	155.1	2.74	1.76	0.0338
Molecular dynamics					
HPβCD:**I**_MD1	N–H···O	164.6	2.73	1.70	0.0448
	N–H···O	155.6	2.88	1.90	0.0328
HPβCD:**I**_MD2	N–H···O	173.6	2.72	1.67	0.0488
	N–H···O	168.2	2.80	1.77	0.0384
HPβCD:**I**_MD3	N–H···O	157.9	2.83	1.84	0.0344
	N–H···O	109.1	2.89	2.37	0.0123

N–H···O contact present in adduct HPβCD:**I**_MD3, this contact presents similar values of ρ_{BCP} in all adducts. This result is interesting because for adducts HPβCD:**I**_CI2 and HPβCD:**I**_MD3, these hydrogen bonds are present outside of the cone defined by HPβCD. Besides, if we compare these contacts with the N–H···O contacts reported in Table 2 for βCD adducts, clearly the N–H···O contact is similar in both sets of adducts. Therefore, the functionalized βCD contains large regions to trap sertraline, but in this situation, hydrogen bonds are not favored, suggesting that these contacts do not drive the stabilization of these inclusion compounds.

3.3 Functionalized β-CD in the separation of sertraline stereoisomers

We used the same approach as that applied to HPβCD:**I** adducts for the **II**, **III** and **IV** stereoisomers in contact with HPβCD. The structures of these adducts are shown in Fig. 8, and additional structures are reported in the ESI.† We again observed that the structures suggested by chemical intuition gave binding energies above those obtained by MD, in the same way as in the previous discussion, and for this reason we will not include adducts suggested by chemical intuition in the following discussion.

The binding energies for adducts between HPβCD and the 4 stereoisomers of SRT are reported in Table 5. For completeness we have included the binding energies reported in Table 3 for the HPβCD:**I** adducts. Let us analyze the most stable adduct for each stereoisomer. In the gas phase we observe practically the

Table 5 Association energies for the adducts between the four stereoisomers of sertraline and HPβCD found by molecular dynamics using the PBE0/6-31G(d,p) method, in the gas phase (ΔE_g, ΔG_g), and in water (ΔE_s, ΔG_s). ΔE contains the zero point energy and the Gibbs energy was estimated at $T = 298.15$ K. All quantities are in kcal mol^{-1}

Adduct	ΔE_g	ΔG_g	ΔE_s	ΔG_s
HPβCD:**I**_MD1	−53.6	−33.7	−17.6	2.4
HPβCD:**I**_MD2	−51.8	−32.1	−15.4	4.2
HPβCD:**I**_MD3	−52.4	−35.0	−18.4	−0.9
HPβCD:**II**_MD1	−52.9	−33.3	−13.1	6.9
HPβCD:**II**_MD2	−51.0	−30.2	−11.8	9.5
HPβCD:**II**_MD3	−50.2	−29.2	−13.6	7.9
HPβCD:**III**_MD1	−53.7	−33.7	−14.6	5.4
HPβCD:**III**_MD2	−49.7	−25.9	−2.5	21.4
HPβCD:**III**_MD3	−42.0	−32.1	−12.6	7.3
HPβCD:**IV**_MD1	−55.9	−32.7	−10.3	12.9
HPβCD:**IV**_MD2	−49.5	−26.0	−3.4	20.1
HPβCD:**IV**_MD3	−48.4	−26.7	−7.2	14.4

same ΔG_g for each adduct, and no trend is observed when solvent effects are taken into account, although we have mentioned the issues with this model for charged systems. Thus, based on the energy, we cannot determine differences in these stereoisomers.

We recognize that there are several energy contributions to the stabilization of βCD inclusion compounds; we can mention hydrogen bonds, van der Waals interactions and electrostatic interactions, all of which are non-covalent interactions. For this reason, we used the NCI to look for the interactions responsible for the stabilization of these systems. The NCI for the structures presented in Fig. 8 is depicted in Fig. 9. From this figure, the role of non-covalent interactions in the formation of these adducts is clear; in particular, the blue regions indicate possible formation of hydrogen bonds. The hydrogen bonds involved in
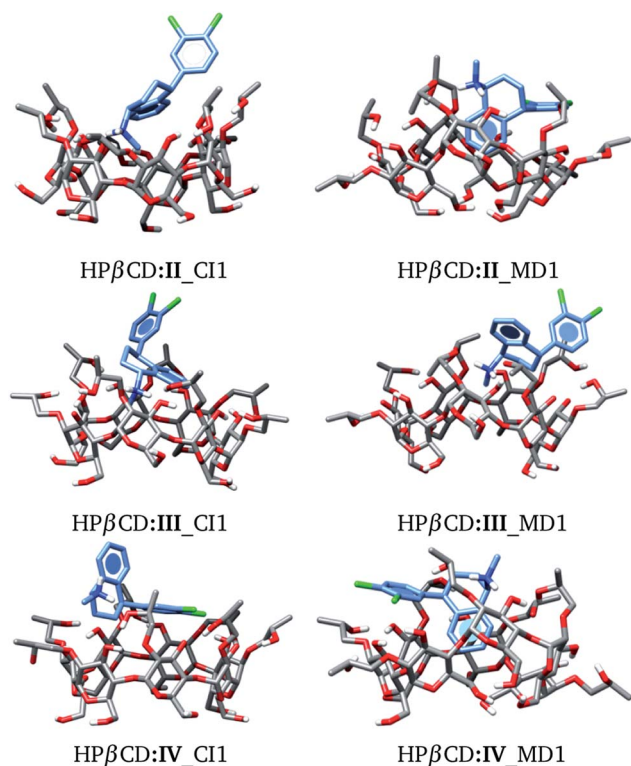
Fig. 8 Conformation of the most stable geometries of inclusion compounds formed between HPβCD and three stereoisomers of sertraline: (**II**) *cis*-(1*R*,4*R*), (**III**) *trans*-(1*R*,4*S*) and (**IV**) *trans*-(1*S*,4*R*).
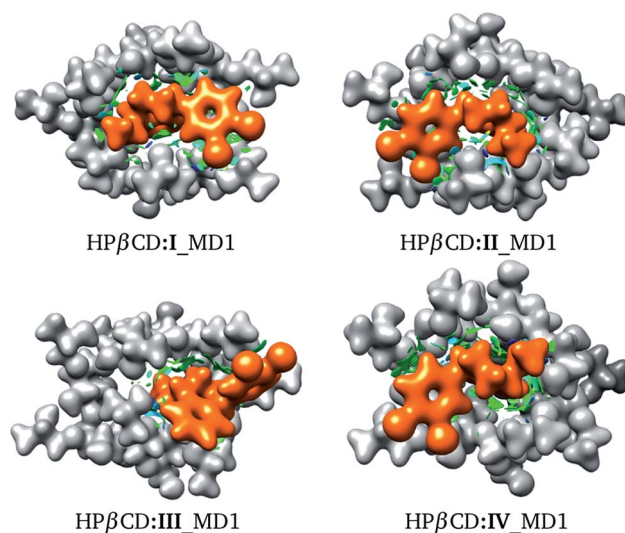
Fig. 9 Electron density with an isosurface of 0.01 atomic units, in white for HPβCD and orange for SRT. Non-covalent interaction index shown as green (weak interactions) and blue (strong interactions) isosurfaces.
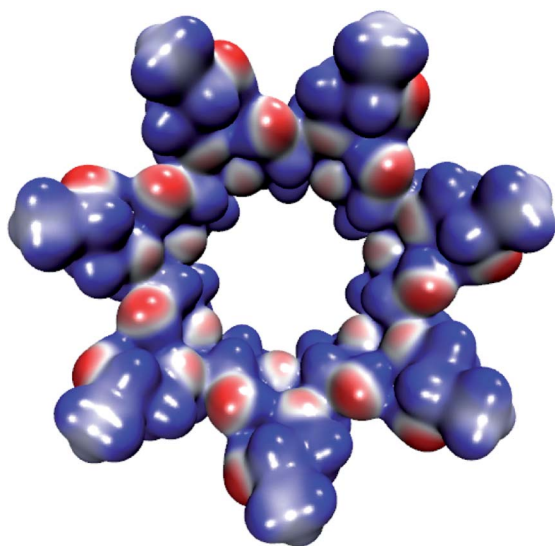
Table 6 Characterization of hydrogen bonds involved in HPβCD:SRT adducts. Distances are in Angstrom and angles are in degrees. The electron density evaluated at bond critical points is reported in atomic units

Adduct	Interaction	θ	R_{DA}	R_{HA}	ρ_{BCP}
Molecular dynamics					
HPβCD:**I**_MD1	N–H⋯O	164.6	2.73	1.70	0.0448
	N–H⋯O	155.6	2.88	1.90	0.0328
HPβCD:**II**_MD1	N–H⋯O	160.6	2.91	1.91	0.0290
	N–H⋯O	159.2	2.85	1.85	0.0333
	N–H⋯O	168.3	2.77	1.73	0.0442
HPβCD:**III**_MD1	N–H⋯O	147.1	2.81	1.89	0.0304
	N–H⋯O	125.6	3.06	2.34	0.0120
HPβCD:**IV**_MD1	N–H⋯O	170.1	2.74	1.70	0.0470
	N–H⋯O	161.5	2.74	1.73	0.0448
	O–H⋯C	158.1	3.27	2.36	0.0140

the HPβCD:SRT adducts were obtained using the QTAIM and their characteristics are reported in Table 6. In many reports, the electron density evaluated at a bond critical point has been used to obtain an idea of the strength of a hydrogen bond. The results in Table 6 show that this property does not follow the same trend as that exhibited by the binding energies. Thus, there are additional interactions aside from hydrogen bonds that stabilize HPβCD:SRT adducts. We must bear in mind that electrostatic interactions are important effects involved in CD inclusion compounds, and for this reason we evaluated the electrostatic potential and the dipole moment of each system involved in HPβCD:SRT adducts.

The molecular electrostatic potential (MEP) of HPβCD is presented in Fig. 10, and the corresponding MEPs for the SRT stereoisomers are depicted in Fig. 11. From Fig. 10 we observe that the negative regions of the MEP for the functionalized CD are localized mainly over the inner regions of the cone. For this
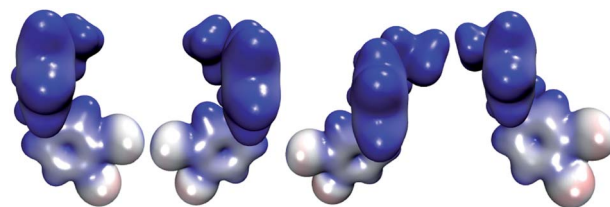
Fig. 11 Molecular electrostatic potentials of the four stereoisomers of sertraline from 0.00 (blue color) to 0.16 (red color) atomic units over an isosurface of the electron density ($\rho(r) = 0.01$ atomic units).

reason, this system attracts species with positive charge towards the wider rim of its cavity. As we mentioned at the beginning of this article, the sertraline used in this study has charge +1. However, there is an important difference between its stereoisomers. Stereoisomers **I** and **II** exhibit almost the same dipole moment, 15.49 and 15.50 debye respectively, which is lower than that presented by stereoisomers **III** and **IV** (20.78 debye for both cases). As we see from Fig. 11, the conformations adopted by the *cis* and *trans* stereoisomers are the main reason for the different dipole moments. Thus, the MEPs suggest that the HPβCD:**III** and HPβCD:**IV** adducts could exhibit bigger binding energies than the adducts containing the **I** and **II** stereoisomers. However, the solvent model used in this article could result in erroneous interpretations of the Gibbs energy changes.

4 Conclusions

The interactions of βCD and HPβCD with sertraline were analyzed using quantum chemistry methods. On the one hand, we concluded that these CDs are suitable species for trapping sertraline since they induce high binding energies, particularly HPβCD. The adducts used to form this conclusion were suggested by molecular dynamics since, without this strategy, the isomers found by chemical intuition exhibited small binding energies. Thus, the second conclusion obtained in this article is that for inclusion compounds with βCD and HPβCD, a molecular dynamics simulation is needed to explore the potential energy surface since this technique allows for distortions in these CDs, and such distortions induce large binding energies. Finally, the molecular electrostatic potential provides insight into the factors involved in the separation of these stereoisomers. However, the solvent model used in this article gives large differences in the binding energies. Thus, the next step of this project is the use of an explicit–implicit model to treat solvent effects.

Conflicts of interest

There are no conflicts to declare.

Acknowledgements

Fig. 10 Molecular electrostatic potential of HPβCD from −0.07 (blue color) to 0.07 (red color) atomic units mapped over an isosurface of the electron density ($\rho(r) = 0.01$ atomic units).

References

1 R. Valle-Cabrera, Y. Mendoza-Rodriguez, M. Robaina-Garcia, J. Ballesteros, J. R. Cordero-Jimenez, N. B. Espinosa-Rodriguez, Y. Sotolongo-Garcia and B. G. Lauria-Horner, *J. Clin. Psychopharmacol.*, 2018, **38**, 454–459.

2 N. A. Fineberg, D. S. Baldwin, L. M. Drummond, S. Wyatt, J. Hanson, S. Gopi, S. Kaur, J. Reid, V. Marwah, R. A. Sachdev, I. Pampaloni, S. Shahper, Y. Varlakova, D. Mpavaenda, C. Manson, C. O'Leary, K. Irvine, D. Monji-Patel, A. Shodunke, T. Dyer, A. Dymond, G. Barton and D. Wellsted, *Int. Clin. Psychopharmacol.*, 2018, **33**, 334–348.

3 S. S. Al-Nimry and M. A. Jaber, *Lat. Am. J. Pharm.*, 2017, **36**, 665–672.

4 S. S. Al-Nimry and M. A. Jaber, *AAPS PharmSciTech*, 2017, **18**, 1190–1202.

5 M. X. Zhou and J. P. Foley, *J. Chromatogr. A*, 2004, **1052**, 13–23.

6 R. N. Rao, M. V. N. Kumar Talluri and P. K. Maurya, *J. Pharm. Biomed. Anal.*, 2009, **50**, 281–286.

7 Q. J. Peng and J. J. Yang, *Chin. Chem. Lett.*, 2014, **25**, 1416–1418.

8 M. L. Reyes-Reyes, G. Roa-Morales, R. Melgar-Fernández, H. Reyes-Pérez and P. Balderas-Hernández, *Chromatographia*, 2014, **77**, 1315–1321.

9 M. Palomar-Pardavé, S. Corona-Avendaño, M. Romero-Romo, G. Alarcón-Angeles, A. Merkoci and M. T. Ramírez-Silva, *J. Electroanal. Chem.*, 2014, **717–718**, 103–109.

10 M. Ceborska, M. Asztemborska and J. Lipkowski, *Chem. Phys. Lett.*, 2012, **553**, 64–67.

11 L. M. Guo, Z. Q. Liu and S. Y. Liu, *Chin. J. Anal. Chem.*, 2005, **36**, 495–497.

12 M. Brusnikina, O. Silyukov, M. Chislov, T. Volkova, A. Proshin, A. Mazur, P. Tolstoy and I. Terekhova, *J. Therm. Anal. Calorim.*, 2017, **130**, 443–450.

13 K. Tang, Y. Chen, K. Huang and J. Liu, *Tetrahedron: Asymmetry*, 2007, **18**, 2399–2408.

14 C. S. Nascimento Jr, J. F. Lopes, L. Guimarães and K. B. Borges, *Analyst*, 2014, **139**, 3901–3910.

15 J. J. Passos, F. B. De Sousa, I. S. Lula, E. A. Barreto, J. F. Lopes, W. B. De Almeida and R. D. Sinisterra, *Int. J. Pharm.*, 2011, **421**, 24–33.

16 J. F. Lopes, C. S. Nascimento Jr, C. P. A. Anconi, H. F. Dos Santos and W. B. De Almeida, *J. Mol. Graphics*, 2015, **62**, 11–17.

17 H. Santillán-Vargas, J. Z. Ramírez, J. Garza and R. Vargas, *Int. J. Quantum Chem.*, 2012, **112**, 3587–3593.

18 G. Nieto-Malagón, J. M. Hernández-Pérez, R. Vargas and J. Garza, *Int. J. Quantum Chem.*, 2012, **112**, 3552–3557.

19 D. T. Thao, K. Nauwelaerts, L. Baudemprez, M. Van Speybroeck, J. Vermant, P. Augustijns, P. Annaert, J. Martens, J. Van Humbeeck and G. Van den Mooter, *J. Inclusion Phenom. Macrocyclic Chem.*, 2011, **71**, 137–147.

20 U. Domanska, A. Pelczarska and A. Pobudkowska, *Int. J. Mol. Sci.*, 2011, **12**, 2383–2394.

21 M. L. Reyes-Reyes, G. Roa-Morales, R. Melgar-Fernández, H. Reyes-Pérez, L. M. Gómez-Oliván, N. González-Rivas, J. Bautista-Renedo and P. Balderas-Hernández, *J. Inclusion Phenom. Macrocyclic Chem.*, 2015, **82**, 373–382.

22 V. Buko, I. Zavodnik, O. Lukivskaya, E. Naruta, B. Palecz, S. Belica-Pacha, E. Belonovskaya, R. Kranc and V. Abakumov, *Chem.-Biol. Interact.*, 2016, **244**, 105–112.

23 M. V. Ol'khovich, A. V. Sharapova, G. L. Perlovich, S. Y. Skachilova and N. K. Zheltukhin, *J. Mol. Liq.*, 2017, **237**, 185–192.

24 M. Terauchi, A. Tamura, S. Yamaguchi and N. Yui, *Int. J. Pharm.*, 2018, **547**, 53–60.

25 S. Adhikari, S. Daftardar, F. Fratev, M. Rivera, S. Sirimulla, K. Alexander and S. H. S. Boddu, *Int. J. Pharm.*, 2018, **545**, 357–365.

26 R. W. Seidel and B. B. Koleva, *Acta Crystallogr., Sect. E: Struct. Rep. Online*, 2009, **65**, o3162–o3163.

27 F. Caruso, A. Besmer and M. Rossi, *Acta Crystallogr., Sect. C: Cryst. Struct. Commun.*, 1999, **55**, 1712–1714.

28 L. Lagardere, L. H. Jolly, F. Lipparini, F. Aviat, B. Stamm, Z. F. Jing, M. Harger, H. Torabifard, G. A. Cisneros, M. J. Schnieders, N. Gresh, Y. Maday, P. Y. Ren, J. W. Ponder and J. P. Piquemal, *Chem. Sci.*, 2018, **9**, 956–972.

29 I. S. Ufimtsev and T. J. Martinez, *J. Chem. Theory Comput.*, 2009, **5**, 2619–2628.

30 A. V. Titov, I. S. Ufimtsev, N. Luehr and T. J. Martinez, *J. Chem. Theory Comput.*, 2013, **9**, 213–221.

31 J. Contreras-García, E. R. Johnson, S. Keinan, R. Chaudret, J.-P. Piquemal, D. N. Beratan and W. Yang, *J. Chem. Theory Comput.*, 2011, **7**, 625–632.

32 E. R. Johnson, S. Keinan, P. Mori-Sánchez, J. Contreras-García, A. J. Cohen and W. Yang, *J. Am. Chem. Soc.*, 2010, **132**, 6498–6506.

33 K. B. Lipkowitz, *Chem. Rev.*, 1998, **98**, 1829–1874.

34 R. Hernández-Esparza, S. M. Mejía-Chica, A. D. Zapata-Escobar, A. Guevara-García, A. Martínez-Melchor, J. M. Hernández-Pérez, R. Vargas and J. Garza, *J. Comput. Chem.*, 2014, **35**, 2272–2278.

35 R. Hernández-Esparza, A. Vázquez-Mayagoitia, L. A. Soriano-Agueda, R. Vargas and J. Garza, *Int. J. Quantum Chem.*, 2019, **119**, e25671.

36 J. C. Cruz, R. Hernández-Esparza, A. Vázquez-Mayagoitia, R. Vargas and J. Garza, *J. Chem. Inf. Model.*, 2019, **59**, 3120–3127.

37 B. P. Hay, D. Zhang and J. R. Rustad, *Inorg. Chem.*, 1996, **35**, 2650–2658.

38 B. P. Hay, D. A. Dixon, R. Vargas, J. Garza and K. N. Raymond, *Inorg. Chem.*, 2001, **40**, 3922–3935.

39 J. J. García, R. Hernández-Esparza, R. Vargas, W. Tiznado and J. Garza, *New J. Chem.*, 2019, **43**, 4342–4348.

40 A. M. Navarrete-López, J. Garza and R. Vargas, *J. Phys. Chem. A*, 2007, **111**, 11147–11152.